Water Research 123 (2017) 49–57

Contents lists available at ScienceDirect

Water Research

journal homepage: www.elsevier.com/locate/watres

Sampling frequency for water quality variables in streams: Systems analysis to quantify minimum monitoring rates

Nick A. Chappell*, Timothy D. Jones, Wlodek Tych

Lancaster Environment Centre, Lancaster University, Lancaster LA1 4YQ, UK

ARTICLE INFO

Article history:
Received 11 January 2017
Received in revised form
11 June 2017
Accepted 17 June 2017
Available online 19 June 2017

Keywords:
Monitoring
Water quality
In-situ measurement
Aliasing
System analysis

ABSTRACT

Insufficient temporal monitoring of water quality in streams or engineered drains alters the apparent shape of storm chemographs, resulting in shifted model parameterisations and changed interpretations of solute sources that have produced episodes of poor water quality. This so-called 'aliasing' phenomenon is poorly recognised in water research. Using advances in *in-situ* sensor technology it is now possible to monitor sufficiently frequently to avoid the onset of aliasing. A systems modelling procedure is presented allowing objective identification of sampling rates needed to avoid aliasing within strongly rainfall-driven chemical dynamics. In this study aliasing of storm chemograph shapes was quantified by changes in the time constant parameter (*TC*) of transfer functions. As a proportion of the original *TC*, the onset of aliasing varied between watersheds, ranging from 3.9–7.7 to 54–79 %*TC* (or 110–160 to 300–600 min). However, a minimum monitoring rate could be identified for all datasets if the modelling results were presented in the form of a new statistic, Δ*TC*. For the eight H^+, DOC and NO_3-N datasets examined from a range of watershed settings, an empirically-derived threshold of 1.3(Δ*TC*) could be used to quantify minimum monitoring rates within sampling protocols to avoid artefacts in subsequent data analysis.

1. Introduction

Storm-driven spikes in dissolved organic matter, nitrate, phosphorus, acidity, pharmaceutical residues and microorganisms in natural streams and engineered drainage systems pose significant risks to human health (Viviano et al., 2014; Carstea et al., 2016; Fauvel et al., 2016). Because stream water quality is typically highly variable through rain-storms (Rozemeijer et al., 2010; Viviano et al., 2014), *attribution of human-induced change* is difficult without continuous, rapid monitoring through sequences of storms (Kirchner et al., 2004; Wade et al., 2012). Furthermore, episodes of poor water quality in streams that induce human health issues or ecological damage may be short-lived during storms (Viviano et al., 2014; Fauvel et al., 2016). Continuous, rapid monitoring of water quality variables in streams (or engineered drainage systems such as sewers) is, therefore, needed to characterise these short-lived but environmentally–significant events (Kirchner et al., 2004; Wade et al., 2012; Viviano et al., 2014; Blaen et al., 2016; Fauvel et al., 2016).

In order to model observed dynamics of particular stream water quality variables through storms (so called 'storm chemographs'), studies have shown that models may need to comprise multiple solute pathways. This arises because:

(1) Different components of the chemograph recession may be associated with different hydrological pathways in the watershed (Barnes, 1939),
(2) Many watersheds exhibit more than one dominant hydrological pathway, and
(3) Over short time scales, stream water quality dynamics are often most strongly associated with hydrological dynamics (Petry et al., 2002; Rozemeijer et al., 2010; Jones and Chappell, 2014; Fauvel et al., 2016).

The fast hydrological pathways can be the ones responsible for producing the 'hot moments' of biogeochemical response in streams, and so must be monitored and modelled at a sufficiently high resolution to capture the salient dynamics during model calibration (and validation). If monitoring (and subsequent modelling) is not undertaken at a sufficiently high sampling rate,

* Corresponding author.
E-mail address: n.chappell@lancaster.ac.uk (N.A. Chappell).

http://dx.doi.org/10.1016/j.watres.2017.06.047
0043-1354/

the *shape of each chemograph* through storms may be altered (in observations and simulated data). When the observations are modelled, changes to the shape of the chemograph are exhibited in changes to model parameters or their derived characteristics capturing features such as the 'flashiness' of the chemograph (seen in for example a Time Constant, *TC*, of a transfer function model of rainfall to solute response). This may cause the modeller to infer a different type of hydrological and/or solute pathway (cf. Barnes, 1939) or pathways with incorrect hydrological and/or chemical characteristics. This shift from the true dynamics by generating modelling artefacts is known as 'aliasing' within Signal Processing Theory. Aliasing is another term for the effects of signal spectrum distortion known as 'spectrum folding' where signals at frequencies higher than $f_N = 1/(2\Delta t)$ are misrepresented in the lower part of the spectrum. Here Δt is the time-step in the observations and f_N is known as Nyquist frequency. Aliasing phenomena are often illustrated with subsampled cyclical data displaying a completely different cycle after subsampling. However, it applies equally to episodic (also called transient or finite length record) time series data (Lathi, 2010), such as storm-induced water quality responses. The phenomenon is little acknowledged in hydrological modelling (Littlewood and Croke, 2013) or hydro-chemical modelling of storm dynamics (Kirchner et al., 2004).

Deployment of high frequency (i.e., sub-hourly monitored) sensors of stream-water for certain water quality variables (e.g., electrical conductivity, pH, temperature, turbidity, dissolved oxygen, fluorescence) has been increasing in recent years (Carstea et al., 2016). Additionally, the number of variables that can be monitored accurately with *in situ* stream sensors has also increased, to include for example, dissolved organic carbon (DOC), dissolved organic matter (DOM), nitrate (NO_3-N) and chlorophyll-a (Blaen et al., 2016; Reynolds et al., 2016). Other technological advances now permit sampling and rapid chemical analysis by colorimetry on stream banks for determinands at trace concentrations, e.g., phosphorus. Consequently, there is now greater opportunity to obtain storm-related chemographs with shapes that are not compromised by under-sampling, and so avoiding sampling-related artefacts in model parameterisations (Jones et al., 2014). There has been much recent research examining the effects of monitoring frequency on the calculation of average solute concentrations (e.g., Reynolds et al., 2016). This research has demonstrated that seasonally-averaged concentrations are relatively insensitive to under-sampling. Littlewood and Croke (2013) have, however, demonstrated for hydrological data that within-storm dynamics and the resultant model parameterisation is very sensitive to the effects of degrading the temporal resolution of the input-output time-series. It is our belief that *no studies have examined systematically the impact of under-sampling stream chemical concentrations upon model parameters capturing chemical concentration changes through storms, and the consequent impact on interpretation of solute pathways.*

While the cost of gaining water quality values using stream sensors is relatively insensitive to the numbers of values collected, unlike water sampling followed by laboratory-based chemical analyses, there are practical/cost constraints on the use of these *in situ* sensor systems. Sensor systems without automated telemetry have a finite local data storage capacity. Greater monitoring rates also result in greater power requirements that may be limited if sufficient renewable energy or mains electricity is unavailable. Consequently, there is considerable value in knowing the *minimum monitoring rate* that does not distort the true shape of chemographs needed for hydro-chemical modelling without creating unnecessary logistical issues for monitoring.

In many headwaters, dynamics in stream water quality may be dominated by short-term changes in the hydrology (i.e., rainfall time-series) via one or more water pathways (Langan and Whitehead, 1987; Littlewood, 1987; Jones and Chappell, 2014). Some process-based models of hydro-chemistry show sensitivity of solute concentration responses to rainstorms, e.g., TNT2-P (Dupas et al., 2016). Rigorous uncertainty analyses applied to process-based models have, however, shown that many are attempting to capture too many processes and so have the downside of producing distributions of the most sensitive model parameters (and related Dynamic Response Characteristics, DRCs) that are too uncertain, i.e., poorly identifiable. This makes process interpretation or quantification of change in DRCs of water quality variables difficult to ascertain. There is, therefore, a compelling argument, for making sure that water quality models are no more complex than warranted by the dynamics observed in the stream water quality variables of interest. Indeed, Langan and Whitehead (1987), Littlewood (1987) and Jones and Chappell (2014) have presented examples systems models based on linear transfer functions where they achieve this using model structures based solely on information from hydrological dynamics.

The aim of this study was to quantify the point at which a reducing monitoring rate would result in a significant shift in model parameters of strongly hydrologically-driven water quality models based on transfer functions, where the identified model for fine monitoring intervals was very well-defined (i.e., high simulation efficiency). These points of change were then analysed to attempt to produce a new procedure for users of water quality sensors (and bank-side analysers) deployed on streams to help identify the minimum monitoring intervals necessary for later modelling (whether by systems analysis or process-based algorithms). Five specific objectives were defined to achieve this aim:

1/ To identify parsimonious transfer function models of example stream water quality variables (based solely on rainfall input) with data monitored at example sites at a high-frequency (i.e. 1, 5 and 15 min). These initial models need to have high simulation efficiency (and so be based upon only a short period of storm-related dynamics) and ideally the DRCs should be physically interpretable.
2/ To subsample the observed time-series of each water quality variable to mimic successively longer monitoring intervals. Parsimonious transfer function models of these data (combined with the rainfall input integrated at the same interval) will be identified using the same numerical tools.
3/ To identify the first significant drift in the key transfer function DRC of the Time Constant (i.e., residence time of response or *TC*) arising from successive models with increasing time-step length.
4/ To attempt to understand and generalise the point at which data and model time-step affects the parameters of systems models based on transfer functions, and by inference the parameterisation of process-based models, and
5/ To outline a recommended procedure for identifying the minimum monitoring intervals necessary for modelling storm-driven, water quality dynamics in streams.

2. Methods

2.1. Selection of illustrative stream water quality datasets

The data utilised consist of those collected continuously at 1-min or 5-min resolution specifically for this study, and existing data collected continuously at 15-min intervals. Hydrogen ion (H^+) concentration (derived from *in situ* pH measurements) is the key chemical variable examined in this study because it is widely

measured and has a long history of high-frequency monitoring (Littlewood, 1987). Example dissolved organic carbon (DOC) and nitrate (NO_3-N) data are also included because of the increasing use of *in situ* UV–Vis sensors (Reynolds et al., 2016). These data are derived from seven watersheds which are all in headwaters, but ranging in basin scale from 0.44 km^2 to 316 km^2 (Table 1). Key watershed details responsible for the observed water quality behaviour (i.e., soil type, geology and land-use) are given in Table 1. Land-use covers both agricultural and forest systems, soils range from acid to alkaline types, and hydrological systems are dominated by either deep or shallow pathways depending on the nature of the solid geology.

The 1-min resolution pH data at the Lower Hafren and Trawsnant watersheds in the UK (Table 1) were measured using a digital differential pH probe (Hach DPS1) connected to a SC200 pH controller recorded on a Campbell Scientific CR1000 data-logger (Jones and Chappell, 2014). The 5-min resolution pH data were monitored in the Baru Watershed (Malaysian Borneo) using a potentiometric pH::lyser pH probe connected to a S::CAN con::cube controller and data-logger (Supplementary Material Section S1). The 15-min resolution pH data from the Pang watersheds (Buckleberry and Tidmarsh monitoring stations in the UK) and Blind Beck watershed (UK) were measured using a YSI 600R sonde fitted with a 6581 pH probe connected to a Campbell Scientific CR10X data-logger (Ockenden et al., 2014). The data for the Pang watersheds were obtained from the NERC Environmental Information Data Centre. In addition to the 1-min resolution pH data from the Trawsnant watershed, 15-min DOC data were obtained using an S::CAN spectro::lyser (Supplementary Material Section S1) locally calibrated to samples analysed (after filtering through 0.45 μm ash-less filter papers) by thermal oxidation and NDIR detector using a Shimadzu TOC-Vcph Analyzer (Jones et al., 2014). The example dataset of 15-min resolution NO_3-N was monitored in the North Fork watershed (USA) using a Hach 'Nitratax plus SC' nitrate sensor connected to a Hach SC200 controller, and obtained from the USGS National Water Information System (http://waterdata.usgs.gov/nwis 1/6/17). The DRCs of these data were obtained by modelling the dynamic relationship between a single rainfall time-series monitored within each watershed and the observed water quality variable (expressed as a concentration). These rainfall data were obtained from a single tipping-bucket raingauge installed within each basin.

2.2. Identification of most parsimonious transfer function model structure and parameters

The primary objective of the systems analysis was to quantify the point at which a reducing monitoring rate would result in a significant drift in key model parameters of strongly hydrologically-driven, water quality models based on linear transfer functions. To reiterate, identification of this point reliably (i.e., with a low degree of uncertainty) requires minimisation of the number of model parameters that are able to reproduce the water quality dynamics with a high simulation efficiency. Such models, where transfer function structures and parameter sets are derived directly from observations within systems analysis, may be described as 'parsimonious models' (Beck, 1987). Within *linear transfer function models of predominantly rainfall-driven, water quality dynamics, the key parameter describing the shape of the storm chemograph and hence the storm dynamics, is the TC of the response* (Langan and Whitehead, 1987; Littlewood, 1987; Jones et al., 2014; Jones and Chappell, 2014). The other parameters of the linear transfer function, namely the pure-time-delay (τ) between the input and its output response, and the steady-state gain of the system, do not affect the shape of the storm chemograph. One approach to identify transfer functions is the Refined Instrumental Variable Continuous-time Box–Jenkins identification (or RIVC) algorithm of Young (2015). RIVC is one of several time-series modelling tools within the CAPTAIN Toolbox for Matlab (Taylor et al., 2007; http://www.lancaster.ac.uk/staff/taylorcj/tdc/download.php 1/7/17) and was applied within this study following a Data-Based Mechanistic (DBM) modelling strategy. The DBM strategy has three stages. First, a range of possible model structures characterising the relationship between rainfall and stream concentration time-series for each water quality variable were identified using RIVC and associated Matlab modelling tools. The feasible model structures and associated parameter sets were derived directly from the observations, and so are defined as *data-based*. Second, many of these models were then rejected after evaluation against a range of mathematical-statistical criteria (Jones et al., 2014). Lastly, any of these models that did not have a feasible hydrological process interpretation were then rejected. Consequently, only those mathematically and statistically sound models accepted as having a hydrological interpretation were defined as *mechanistic* and therefore, described as Data-Based Mechanistic models.

To illustrate how RIVC-defined model parameters are used to derive the *TC* of the rainfall-driven concentration responses, an example model structure for 1-min monitored time-series of nitrate (NO_3-N) concentrations produced from two parallel hydrological pathways is presented. In continuous-time transfer-function form for 1-min monitored NO_3-N concentration, this can be given as:

Table 1
Characteristics of watersheds included in this study.

Stream	basin area (km^2)	soil types	geology	land-use & land-cover	Reference
Baru, Malaysia	0.44	Alisol	Neogene mudstones and sandstones	Lowland dipterocarp rainforest	Chappell et al. (2012)
Trawsnant, UK	1.21	Histosol, podzol, gleysol	Lower Palaeozoic shales, mudstones, greywackes and grits	Coniferous plantation	Jones and Chappell (2014)
Lower Hafren, UK	3.6	Podzol, histosol, cambisol and stagnogley	Lower Palaeozoic slate, mudstone, greywackes and sandstone	Coniferous plantation	Bell (2005)
Blind Beck, UK	8.8	Stagnosol, leptosol, cambisol, gleysol	Triassic sandstone, Carboniferous limestone	Agriculture (improved and unimproved pasture)	Ockenden et al. (2014)
Pang at Buckleberry, UK	110	Leptosol, cambisol, luvisol, planosol	Cretaceous chalk, Paleogene sediments	Agriculture (arable and pasture)	Wade et al. (2012)
Pang at Tidmarsh, UK	150	Leptosol, cambisol, luvisol, planosol	Cretaceous chalk, Paleogene sediments	Agriculture (arable and pasture)	Wade et al. (2012)
North Fork Maquoketa, USA	316	Luvisol, acrisol	Ordovician shale, carbonate, dolomitic shale and dolomite	Agriculture (arable)	Witzke (1998)

$$NO_3 - N = \left(\frac{\beta_0 s + \beta_1}{s^2 + \alpha_1 s + \alpha_2}\right) e^{-s\tau} R \;\; ; \;\; s \sim \frac{d}{dt} \quad (1)$$

where NO_3-N is the nitrate concentration (μeq/L monitored every minute), R is the rainfall (mm/1-min), τ is the pure time delay between R and an initial NO_3-N response (given in number of 1-min intervals), α_1 and α_2 the parameters that jointly capture the rate of watershed soil-water exhaustion or residence time of response (/1-min), β_0 and β_1 the parameters (jointly with the α_1 and α_2 parameters) that capture the magnitude of NO_3-N gain (μeq/L NO_3-N 1-min/mm), t is time in 1-min periods, and s is the Laplace operator (Young, 2015). Prior to DRC derivation, a model with two parallel hydrological pathways should be decomposed by partial fraction expansion into two parallel, first-order transfer functions:

$$NO_3 - N = \frac{\beta_f}{s - \alpha_f} e^{-s\tau} R + \frac{\beta_s}{s - \alpha_s} e^{-s\tau} R \quad (2)$$

where α_f and α_s are the parameters representing the rate of watershed soil-water exhaustion of NO_3-N or residence time of the fast and slow components of response (/1-min), and β_f and β_s the parameters capturing the magnitude of the fast and slow solute transport components, respectively (μeq/L NO_3-N 1-min/mm). The α_f and α_s model parameters can then be interpreted in terms of the DRCs of the TC of the fast solute pathway and slow solute pathway. For the fast path this is given as:

$$TC_{fast} = \frac{\Delta t}{\alpha_f} \quad (3)$$

where Δt is the time-step in the observations (1-min in this example).

2.3. Quantification of time-step effects: developing a new methodology

To quantify how reducing the sampling interval effects stream chemograph shape (and parameters describing the relationship between rainfall and the storm chemograph), the model derived from the highest frequency sampling should first be simulated with a high efficiency. The objective function used in this study was the Nash-Sutcliffe Efficiency (E or R_t^2: Young, 2015), and only models with an $R_t^2 > 0.90$ at the highest measurement frequency were used for the subsampling exercise. To ensure this, only short periods of example water quality data covering two to five rainstorms were modelled (Table 2). These periods comprised of between 300 and 12,000 contiguously measured water quality values to demonstrate the applicability of the approach to relatively short sets of data. In order to mimic successively longer monitoring intervals, new water quality datasets were produced by taking time factors of the 300 to 12,000 measured values (Table 2). The rainfall data monitored at the same intervals as the original concentration data were then integrated over the new longer monitoring intervals to permit the rainfall to concentration modelling (i.e. the rainfall and concentration data need the same time-step within the transfer function identification process).

Optimal model structure was identified initially for first-order transfer function models (i.e. models with one α value and hence one TC value) using the highest R_t^2. The data were then applied to estimate second-order model structures. Where the resultant R_t^2 was higher than that for first-order models applied to the same data, these models were then accepted as superior but only if they also met a range of evaluation criteria. These criteria included: i) changes of less than +1.0 in the Young Information Criterion (*YIC*), ii) a transfer function without complex roots, i.e., no oscillatory behaviour in the impulse response function, and iii) the sign (±) of the two denominator roots of the transfer function polynomials were both negative (see further explanation in Jones et al., 2014). This procedure was repeated for third-order models.

The next step in identifying the minimum monitoring rates was visualisation of the simulated chemographs at the successively subsampled monitoring intervals to identify changes in storm chemograph shape qualitatively. The derived TC values for each example watershed dataset were then plotted against the mimicked sampling interval. To identify the subsampling interval where the sole TC or fastest TC of higher-order models was substantially affected (i.e., first systematic drift) by the reduced sampling rate, a new evaluation criterion derived from empirical observation of preliminary results was calculated:

$$\Delta TC = \frac{\max(TC_O, TC_i)}{\min(TC_O, TC_i)} \quad (4)$$

where TC_O is the first-order model TC value or TC_{fast} value of higher-order models derived from the original 1, 5 and 15 min water quality observations (h), and TC_i is the TC (or TC_{fast}) value derived as each successively subsampled water quality data-set was modelled (h). This ΔTC criterion is, therefore, a ratio of the larger value of pairs of TC_O and TC_i values to that of the smaller, so that the magnitude of change can be calculated irrespective of the direction of drift. These ΔTC values were then plotted against the mimicked sampling interval to help quantify:

i/ The magnitude of ΔTC associated with the first substantial drift in value as sampling interval is reduced by factors of the original interval (Table 2),
ii/ The mimicked monitoring interval (in h) at which subsampling by factors has resulted in the first substantial shift in derived TC_i from TC_O (T_{drift}), and the longest interval resulting in a TC_i that has not drifted substantially from TC_O ($T_{acceptable}$ or T_{acc}),
iii/ The mimicked monitoring intervals T_{acc} and T_{drift} expressed as a percentage of the TC_O (in part to evaluate the tentative 17% TC_O 'rule' suggested by Young, 2010),
iv/ An analytical protocol for use by others to identify objectively a minimum monitoring interval that does not alias dynamics within strongly hydrologically-driven, water quality models,
v/ If the effect of aliasing on a key DRC of water quality dynamics (namely TC) can be generalised, and
vi/ If a common minimum measurement interval (h) can be identified for the example data, to provide a first estimate for those authorities deploying water quality sensors or bank-side analysers for routine monitoring, where the capacity to undertake any system analysis is limited.

3. Results and discussion

3.1. Identification of optimal models of stream water quality dynamics through storms

The optimal linear transfer function models of hydrologically-driven, water quality dynamics identified for the selected short period of storms are given in Table 3. For the Baru basin as an example, the top 20 identified models based on the primary R_t^2 criterion are shown in Supplementary Material Table S1, with the optimal model selected after evaluation against the secondary criteria (see 2. Methods and Table 2) shown in bold. All transfer function models were identified using the RIVC algorithm within version 7.5 of the CAPTAIN Toolbox implemented in version R2013a

Table 2
Data periods, water quality variables and subsampled intervals.

Site	variable	Period	values	resolution (min)	subsampled intervals, all factors of number of values in modelled dataset at highest resolution (min)
Trawsnant	H^+	08/10/2014 20:22–11/10/2014 11:43	3800	1	1, 2, 5, 10, 20, 25, 40, 50, 76, 95, 100, 152, 190, 200
Hafren	H^+	20/12/2014 22:10–29/12/2014 22:35	12000	1	1, 2, 5, 10, 20, 30, 40, 50, 60, 80, 100, 150, 300, 400, 500, 600, 750, 800
Baru	H^+	16/06/2015 12:44–21/06/2015 10:00	1408	5	5, 10, 20, 40, 55, 80, 110, 160, 220, 325[a]
Blind Beck	H^+	04/10/2008 04:00–18/10/2008 18:00	1400	15	15, 30, 60, 75, 105, 120, 150, 300, 375, 420
Pang at Tidmarsh	H^+	07/12/2006 00:30–10/12/2006 03:15	300	15	15, 30, 45,60, 75, 90, 150, 180, 225, 300
Pang at Buckleberry	H^+	07/01/2004 13:45–22/01/2004 03:30	1400	15	15, 30, 60, 75, 105, 120, 150, 300, 375, 420, 525[a], 600[b], 750[b], 840[b], 1050[b], 1500[b]
Trawsnant	DOC	27/05/2013 11:45–04/06/2013 19:45	800	15	15, 30, 60, 120, 150, 240, 300, 375, 480
North Fork	NO_3-N	20/06/2012 01:15–17/07/2012 23:00	2680	15	15, 30, 60, 75, 120, 150, 300, 600

[a] Model failed evaluation criteria (e.g., negative *fast%*; TC_i has an imaginary number) - see 2. Methods.
[b] No model identifiable.

Table 3
Model structure, parameters (α_1, α_2, β_0, β_1,τ) and model evaluation measures (R_t^2, *YIC*) for the optimal rainfall to stream concentration system-models.

Site	variable	interval (min)	model[a]	α_1 (α_f)	α_2	β_0	β_1	τ (min)	R_t^2	*YIC*
Trawsnant	H^+	1	[1 1262]	0.00096		5.5383		262	0.9054	−12.19
Hafren	H^+	1	[1 1 0]	0.00063		1.26400		0	0.9094	−13.15
Baru	H^+	5	[2 2 14]	0.02533 (0.02663)	1.93E-05	0.30547	0.000117	70	0.9424	−8.50
Blind Beck	H^+	15	[2 2 17]	0.02985 (0.07694)	7.16E-05	0.085547	0.000437	255	0.9037	−6.14
Pang at Tidmarsh	H^+	15	[1 1 22]	0.00961		0.000155		330	0.9726	−12.00
Pang at Buckleberry	H^+	15	[2 2 8]	0.01258 (0.00148)	1.09E-05	0.001573	2.44E-06	120	0.9334	−5.37
Trawsnant	DOC	15	[1 1 13]	0.01250		0.27863		195	0.9856	−13.60
North Fork	NO_3-N	15	[1 1 98]	0.00195		0.23143		1470	0.9008	−11.66

[a] Model structure is given as [denominators, numerators, pure time delays] in Eq. (1).

of the Matlab programming environment. These purely linear transfer function models were able to capture more than 90 percent of the storm-related dynamics in the concentration time-series (Table 3), thereby achieving the first objective. The high efficiency is also demonstrated in the correspondence of the simulated concentration time-series' and the observed data (Fig. 1ac and Supplementary Material Fig. S1-S8). The high efficiency shows the dominance of the rainfall control on storm chemographs in the selected headwater streams through short sequences of storms, as demonstrated previously by Petry et al. (2002), Rozemeijer et al. (2010), Jones and Chappell (2014) and Fauvel et al. (2016). Minor additional effects of nonlinearity on the dynamics of these short time-series, were not simulated because of the adverse impacts of: i/adding additional model parameters to the uncertainty in the critical *TC* values, and ii/the adverse impact on the hydro-chemical interpretation of the *TC* values (Jones et al., 2014).

The high model efficiency, necessary to attribute change in model parameters to under-sampling rather than model structural inadequacies, required second-order model structures for three out of the seven datasets. Such second-order structures of hydro-chemical response in streams can be interpreted as the presence of two dominant solutes pathways delivering chemicals to streams, perhaps related to two hydrological pathways. These second-order models have five model parameters (i.e., α_1, α_2, β_0, β_1,τ) against the three model parameters of the first-order transfer function models (i.e., α_1, β_0, τ). The effect of an increase in model parameters can be seen in the deterioration of the *YIC* model-evaluation measure (i.e., a less positive value: Supplementary Material Tables S2–S9). As the continuous-time transfer function models presented here are identified directly from the information content of the observations, fewer parameter numbers are needed when compared with other types of model that have a simplified model structure, but still require 10–30 model parameters (e.g., Dupas et al., 2016). It would be difficult to use models utilising so many parameters to identify change in one model parameter (e.g., α_1) as sampling is changed, because of parameter identifiability issues.

The systems models based on transfer functions identified within this study may be considered to be robust for the selected periods because they are able to capture the dominant dynamics in rainfall-solute systems with a very wide range of residence or exhaustion time, gain and pure-time-delay parameters, in addition to identifying model order (Jones et al., 2014; Jones and Chappell, 2014). The rate of exhaustion in the fastest component of solute response to a rainfall input varies from a flashy 0.02663/1-min Baru H^+ response (α_f) to a very slow 0.00195/15-min NO_3-N response in the North Fork watershed (α_1; Table 3). This equates to a very short residence time of response of 3.4 h for the Baru H^+ response (TC_{fast}), and a relatively long residence time of 128.0 h for the North Fork NO_3-N response (*TC*). The sensitivity of the fastest stream concentration response to a rainfall input (β_0) varies from 0.000155 μeq/L H^+ 1-min/mm in the chalk-dominated Pang (Tidmarsh) watershed to a very sensitive 5.5383 μeq/L H^+ 1-min/mm response in the upland acidic Trawsnant basin. Further, the delay between a rainfall input and an initial concentration response in the stream (τ) varies from no delay (i.e., Hafren H^+) to response delayed by 24.5 h (i.e., North Fork NO_3-N). *While the examples are primarily of H^+ response, the two additional examples (NO_3-N and DOC) show that the approach can be applied equally to other water quality variables where they are*

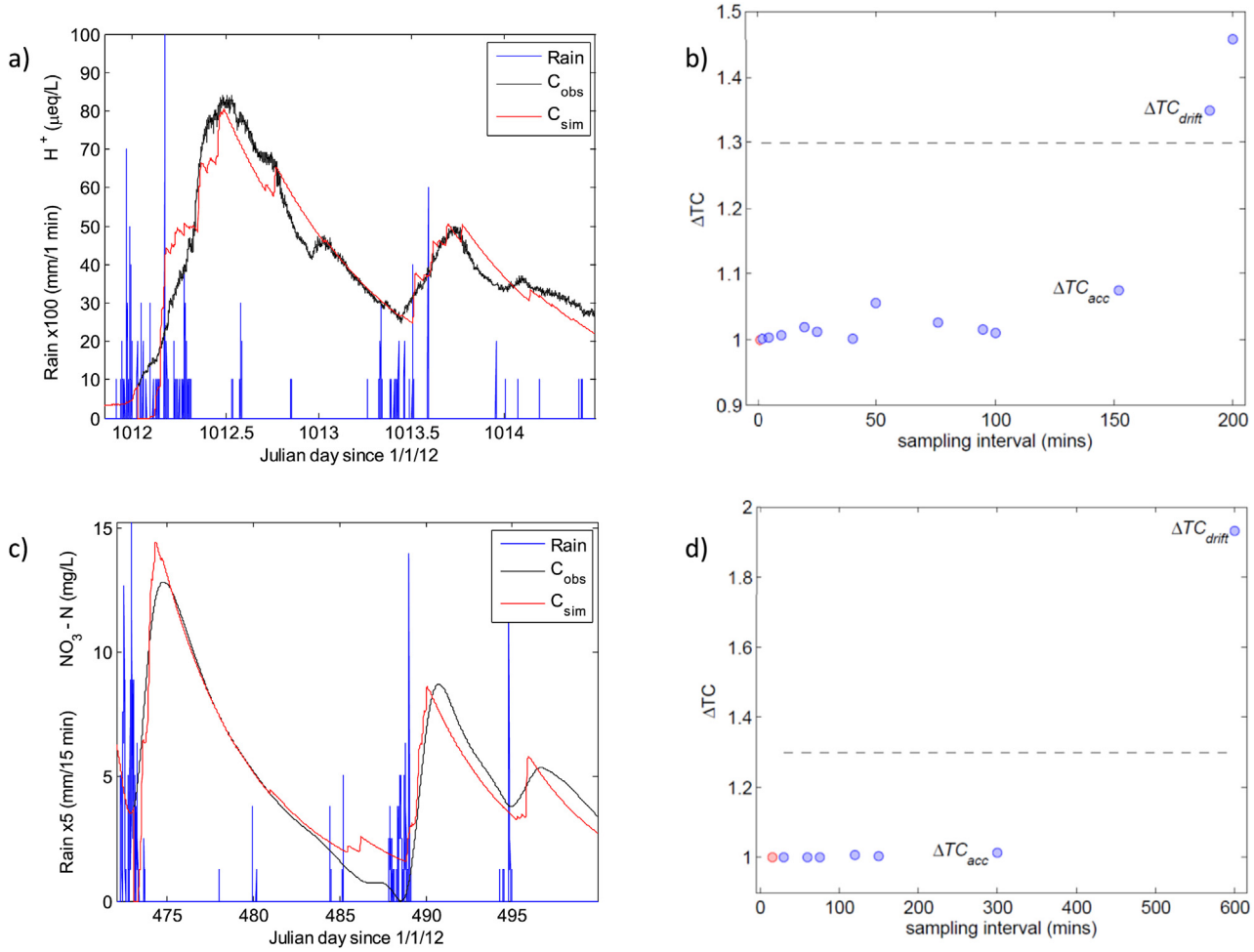

Fig. 1. Simulated versus observed concentration time-series' (C_{sim} and C_{obs}, respectively) for two example datasets monitored at a high frequency, together the derived Δ*TC* change criterion for the optimum model for these data and after successive subsampling: a) and b) are based on the 1-min H^+ concentration time-series from the Trawsnant basin; c) and d) 15-min NO_3-N from the North Fork basin. Scaled rainfall time-series are also shown in a) and c). The Δ*TC* for the observed high frequency data are shown in b) and d) with an filled red circle, and for the subsampled data with filled blue circles, while the threshold of change in Δ*TC* of 1.3 is shown as a broken line. (For interpretation of the references to colour in this figure legend, the reader is referred to the web version of this article.)

strongly hydrologically-driven (Table 3).

3.2. Identification of thresholds of change in parameters of water quality dynamics

Having derived optimal models of the rainfall-concentration dynamics, the water quality datasets used to derive these models were subsampled by taking time factors of the 300 to 12,000 measured values (Table 2), and rainfall data integrated to the same time-intervals. The RIVC algorithm was then used to attempt to identify similarly optimal models for these sub-sampled data (objective 2). Feasible models could be identified for most of these progressively thinned datasets (Table 2) and their structures and efficiencies are shown in Supplementary Material Tables S2-S9. The TC_i values for models from iterations of the reduced sampling rate were derived using Eq. (3). These TC_i values relate to single-pathway models or the fast component of decomposed parallel second-order models (Eq. (2)). The Δ*TC* values (Eq. (4)) for each iteration were then calculated and also presented in Supplementary Material Tables S2–S9. Only one dataset (H^+ monitored at Buckleberry) produced no identifiable models after thinning beyond a certain sub-sampling time (Table 2 and Supplementary Material Table S7). Further, the model for this dataset at a 525-min sampling time produced a TC_i with a large imaginary number component and so was rejected on the basis of the DBM evaluation criteria. The second-order model for 325-min sampling of the Baru watershed H^+ data produced a negative *fast%* (see Eq (8) in Jones et al. (2014). value and was also rejected on the basis of the DBM evaluation criteria. All other simulations produced feasible models (Supplementary Material Tables S2–S9) that met the DBM evaluation criteria.

For each watershed, the Δ*TC* values were plotted against their respective subsampling interval (Fig. 1bd and Supplementary Material Figs. S17–S24). Using these plots the point at which Δ*TC* began to drift systematically from the initial value of unity was somewhere between the sub-sampling intervals of 152–190 min (Trawsnant H^+), 600–750 min (Hafren), 110–160 min (Baru), 105–120 min (Blind Beck), 180–225 min (Pang at Tidmarsh), 300–375 min (Pang at Buckleberry), 240–300 min (Trawsnant DOC), and 300–600 min (North Fork). The initial value in these ranges equates to the TC_{acc} and the second value the TC_{drift} (Table 4). From Fig. 1bd (and Supplementary Material Figs. S17–S24), it can be seen (purely empirically) that for all watershed datasets studied a Δ*TC* value of 1.3 lies within the ranges of these change points (Fig. 1bd), i.e., the point where the TC_i values differ from TC_O values by a factor of 1.3 when the larger of the two values is presented as a

Table 4
Longest sampling interval prior to the systematic drift in the ΔTC measure (T_{acc}), together with the associated values of the time constant and change criterion for this value and when change first identified (T_{drift}). Values are presented to four decimal places to permit direct comparison with the values in Supplementary Material Tables S2–S9.

site	variable	sampling interval		TC		ΔTC	
		T_{acc} (min)	T_{drift} (min)	TC_{acc} (h)	TC_{drift} (h)	ΔTC_{acc}	ΔTC_{drift}
Trawsnant	H^+	152	190	16.1068	18.8288	1.0740	1.3484
Hafren	H^+	600	750	26.9490	14.9136	1.0194	1.7726
Baru	H^+	110	160	2.9058	1.5908	1.1684	2.1343
Blind Beck	H^+	105	120	7.6200	6.2776	1.2053	1.4631
Pang at Tidmarsh	H^+	180	225	24.6048	8.2917	1.0573	3.1649
Pang at Buckleberry	H^+	120	300	22.3922	13.7787	1.0431	1.5580
Trawsnant	DOC	240	300	16.0387	12.2864	1.2475	1.6285
North Fork	NO_3-N	300	600	129.7649	247.2637	1.0141	1.9323

ratio of the smaller (Eq. (4)). After the point where ΔTC began to drift systematically from the initial value of 1.0000 (i.e., TC_O/TC_i and TC_i/TC_O), the slope of the chemograph recessions were visually different (Supplementary Material Fig. S9–S16), as expected (see Fig. 1d vs Fig. 1c in Kirchner et al., 2004). While there is an apparent consistency in the onset of aliasing identified using the new ΔTC criterion, such consistency was not seen in the R_t^2 or YIC criteria when changing sampling intensity (Supplementary Material Tables S2–S9). The YIC is a measure of the uncertainty in the parameterisation. As the largest shifts in YIC did not occur at the point of systematic ΔTC drift (Supplementary Material Tables S2–S9), adding lengthy parameter uncertainty estimation would not give substantial improvements for the potential end-users to the procedures outlined.

The sampling interval for the beginning of the systematic drift (i.e., a range between T_{acc} and T_{drift}; see Fig. 1bd) can be expressed as a percentage of the TC_O. This was calculated to be between 15 and 18% (Trawsnant H^+), 38–47% (Hafren), 54–79% (Baru), 20–25% (Blind Beck), 12–14% (Pang at Tidmarsh), 23–29% (Pang at Buckleberry), 20–25% (Trawsnant DOC), and 3.9–7.7% (North Fork NO_3-N) of the TC_O. Young (2010) tentatively suggested that the TC_O value might be used to set the minimum monitoring interval to avoid aliasing the dynamics of natural input-output systems. The findings from our analysis do indeed show an association between the TC value and the sampling interval at which dynamics become aliased (Fig. 2). Young (2010) tentatively suggested that minimum sampling intervals might be set at approximately one sixth of the TC_O, which is equivalent to 17% of the TC_O. In some contrast, our findings show that while there is an underlying link with the TC, the points of change vary from a sampling rate of less than 10% of the TC_O to one greater than 50% of the TC_O. These variations are likely to occur as stream water quality monitoring rate is reduced because of the impact of characteristics that are specific to each dataset (i.e., watershed, hydro-chemical variable, sensor type etc.). Differences in data characteristics result from: i/the differential effects of integrating the hyetographs with different properties over successively larger intervals (Kretzschmar et al., 2014), ii/the effects of different degrees of sensor or calibration noise within the observed chemographs (Lepot et al., 2016), and iii/the differential ability of the modelling tools to simulate input-output dynamics as the information content deteriorates with reduced monitoring interval (Littlewood and Croke, 2013).

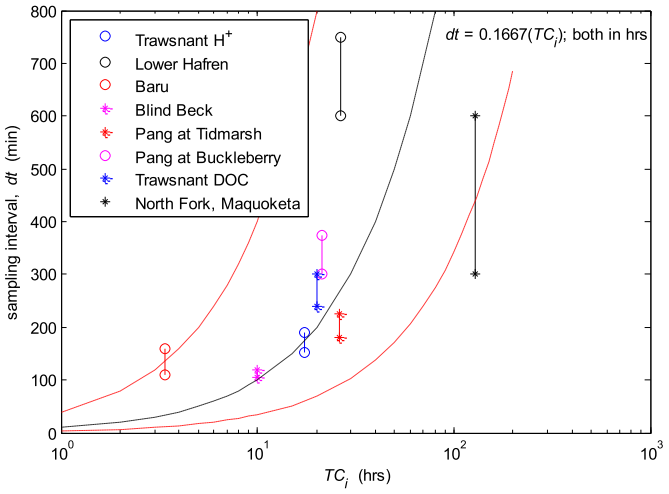

Fig. 2. Onset of systematic drift in dynamics ('aliasing'), lies somewhere between the TC_{acc} and TC_{drift} values for each site (shown with a line between each pair of values). The lower value of each pair is always TC_{acc}, and higher value TC_{drift}. The positive relationship between sampling interval (dt) and 16.67% of TC_o (following the tentative suggestion of Young, 2010) is shown with a broken black line. The observed variability about this relation is also shown by fitting a linear model through the middle of the pair of values furthest from the trend line (broken red lines). Due to the very wide range of TC_i exhibited by the example data, the TC_i axis is presented on a lognormal scale. (For interpretation of the references to colour in this figure legend, the reader is referred to the web version of this article.)

3.3. Recommendations for defining minimum monitoring rates of stream water quality variables

To reiterate, this work was stimulated by two recent trends. Firstly, there has been an increase in deployment of stream sensors and bank-side analysers producing water chemistry data at a high frequency (sub-daily) resolution. Secondly, the impact of under-sampling of water quality variables on the reliability of watershed modelling is beginning to emerge in system analysis (Jones et al., 2014; Reynolds et al., 2016). Given these two drivers, this study sought to develop an example protocol for use by others in designing stream monitoring systems that give data for subsequent modelling (whether using system analysis or process models) that is less affected by under-sampling issues. In this first attempt at deriving a modelling-relevant monitoring protocol for such systems, eight example datasets observed at a high-frequency were selected from watershed systems exhibiting very flashy to damped concentration responses in systems driven primarily by rainstorm inputs. These example systems also exhibited a diverse range of dominant water pathways and hence potential solute pathways, from shallow tropical systems to temperate systems with deep, rock aquifers.

In broad terms, our approach using high-frequency observations combined with systems analysis based on linear transfer function modelling, has demonstrated that the storm-related dynamics within stream concentration time-series may be unaffected by sampling intensity at least up to rates of every 1 h (i.e., T_{acc} in Table 4). Limiting water quality sensing data storage to once every hour would have significant advantages for data logger memory

and power consumption. These findings were primarily based upon H^+ concentration time-series, and such a rate would not be expected to be sufficient for modelling water quality variables primarily carried by overland flow, such as turbidity and phosphorus concentration. Moreover, the actual minimum sampling rates for the data studied (primarily H^+ but with DOC and NO_3-N) varied substantially from less than 120 min to greater than 600 min (Table 4). This range in minimum sampling rate is seen to be important if one considers recent attempts at higher frequency stream water sampling (namely every 7 h) for subsequently laboratory analyses (Halliday et al., 2013).

Young (2010) tentatively suggested that the minimum sampling rate for streamflow and water quality response could be estimated from a fixed proportion of the residence time of the stream's response to rainfall. This proportion was said to be approximately one sixth (i.e. 17%) of the time constant (TC_O) of an input-output transfer function linking the two variables. While our findings confirm the worth of the time constant in identifying minimum sampling rates, the relationship with the time constant varied considerably between our water quality examples. While the Baru H^+ dataset required sampling at a rate approaching the time constant (i.e. 54–79% TC_O), the North Fork NO_3-N dataset required a much higher degree of sampling within the period defined by the time constant (i.e. 3.9–7.7% TC_O). This means that those needing to determine minimum monitoring rates of stream water quality variables at their specific sites would need to undertake approaches such as the iterative combined sub-sampling and modelling procedure outlined here.

The sampling intervals above which the storm-related water quality dynamics (expressed in terms of *TC)* drift from the true values due to the phenomenon of 'aliasing', were clearly identifiable by the new procedure outlined here (Fig. 1bd). This procedure might be considered by others seeking to optimise their monitoring strategies provided that they, 1/can show that the dynamics in the water quality time series of interest are dominated by the dynamics in one controlling variable (e.g., rainfall), 2/obtain an initial period of high-frequency, stream water quality data (with parallel rainfall data) for a short sequence of contiguous storms, 3/are able to simulate the high-frequency dynamics using parsimonious transfer-function based approaches (e.g. RIVC, IHACRES, MATLAB-BJ), 4/mimic the effects of reducing sampling intervals by successively sub-sampling the original observations and re-applying the same modelling tools, and 5/use the derived model parameters to identify systematic drift within the empirical ΔTC criterion. Ideally, each concentration value within the high-frequency data should have high accuracy against laboratory measured values. Sensor inaccuracies cause noise within the time-series that affect the uncertainty and true identification of model parameters and consequently derived values such as *TC*. Consequently, the algorithms chosen to identify optimal transfer function parameters need to incorporate routines that mitigate the effects of noise, such as those within RIVC (Young, 2015). Similarly, the model identification routines should have the capacity to identify efficient model structures with the least parametric uncertainty, so that sampling related changes in *TC* can be seen above model error. The parallel rainfall data needs to be representative of that which generates the concentration responses. Consequently, as watershed size increases the rainfall time-series used as input for the models should be based upon spatial integration of ever larger numbers of raingauges.

For the range of predominantly rain-driven, water-chemistry dynamics exhibited by our examples, a common ΔTC value seemed to define the minimum sampling interval for all datasets. An apparent threshold could be set at a ΔTC value of 1.3 and apply to all datasets examined. Whether, this apparent threshold is present after application of these procedures to other water quality variables (physical, biological and chemical: Fauvel et al., 2016) or different watershed settings (e.g., sewers: Carstea et al., 2016; Lepot et al., 2016) should be explored at time of application or in future research studies.

4. Conclusions

This research has demonstrated the value of a systems analysis technique based on transfer functions in helping to identify the monitoring frequencies required for water quality variables in rainfall-driven environmental systems. Specifically, the work revealed that:

- Where the dynamics of stream water quality are dominated by rainfall dynamics and the variables measured at a high frequency (1–15 min), then stream water quality may be able to be modelled using transfer functions with rainfall input data alone.
- These high frequency data were sub-sampled to mimic less frequently sampled datasets. The rainfall-driven concentration dynamics, expressed as parameters of the transfer function based systems model, were shown to be distorted as sampling reduced beyond once every 1 h to 10 h, depending on the chemical variable and location.
- The distortion in model parameters, due to under-sampling of stream water quality, is known as 'aliasing' in systems analysis and such parameter shifts affect the interpretation of the processes (physical, chemical or biological) in models of biogeochemistry, hydro-chemistry, or hydrology.
- It has been suggested previously that the onset of aliasing might be associated with the time constant parameter of linear transfer function models of environmental systems. This study presents the first evidence that aliasing is associated with *shifts* in the time-constant parameter (*TC*) identified from systems analysis of high frequency water chemistry data. From a Signal Processing perspective, the shift in the *TC* reflects a shift or distortion of the signal spectrum. From a water quality perspective, the shift in the *TC* reflects a distortion in the shape of the storm chemograph. A new empirically-derived statistical measure, $1.3(\Delta TC)$, was derived for headwaters with a wide range of rainfall-derived chemical dynamics, and indicates the minimum sampling required to avoid such distortions and so errors in process interpretations arising from subsequent modelling of inadequately sampled data.
- With the availability of a short sequence of high frequency water chemistry data, this statistical measure, $1.3(\Delta TC)$, could be derived using widely available systems analysis techniques based on linear transfer functions (not just the RIVC algorithm presented here), and used as a guide to establish minimum monitoring rates for long-term sampling of natural streams or indeed any strongly rainfall-controlled drainage system (e.g., sewers, urban drains)
- Further evaluation of the approach is required to assess its wider applicability for designing monitoring protocols for a much broader range of water quality characteristics (including physical and biological properties) than could be presented in this initial study.

Acknowledgements

This study was funded by Natural Environment Research Council grants NE/J014826/1 [DURESS-Lancaster project within the NERC Biodiversity & Ecosystem Service Sustainability programme] and NE/I022450/1 [WGhats-Capacity within the NERC Changing Water Cycle programme]. The authors thank landowners and

Yayasan Sabah Group for access to the Trawsnant, Hafren and Baru research basins. M. Ockenden is thanked for the collection of Blind Beck basin data.

Appendix A. Supplementary data

Supplementary data related to this article can be found at http://dx.doi.org/10.1016/j.watres.2017.06.047.

References

Barnes, B.S., 1939. The structure of discharge recession curves. Trans. Am. Geophys. Union 4, 721–725.
Beck, M.B., 1987. Uncertainty in water quality models: a review of the analysis of uncertainty. Water Resour. Res. 23, 1393–1442.
Bell, J., 2005. The Soil Hydrology of the Plynlimon Catchment. Institute of Hydrology, Wallingford, U.K.
Blaen, P.J., Khamis, K., Lloyd, C.E.M., Bradley, C., Hannah, D., Krause, S., 2016. Real-time monitoring of nutrients and dissolved organic matter in rivers: capturing event dynamics, technological opportunities and future directions. Sci. Total Environ. 569–570, 647–660.
Carstea, E.M., Bridgeman, J., Baker, A., Reynolds, D.M., 2016. Fluorescence spectroscopy for wastewater monitoring: a review. Water Res. 95, 205–219.
Chappell, N.A., Bonell, M., Barnes, C.J., Tych, W., 2012. Tropical cyclone effects on rapid runoff responses: quantifying with new continuous-time transfer function models. In: Webb, A.A., Bonell, M., Bren, L., Lane, P.N.J., McGuire, D., Neary, D.G., Nettles, J., Scott, D.F., Stednik, O.J., Wang, Y. (Eds.), Revisiting Experimental Catchment Studies in Forest Hydrology, vol. 353. IAHS Press IAHS Publ., Wallingford, pp. 82–93.
Dupas, R., Salmon-Monviola, J., Beven, K., Durand, P., Haygarth, P.M., Hollaway, M.J., Gascuel-Odoux, C., 2016. Uncertainty assessment of a dominant-process catchment model of dissolved phosphorus transfer. Hydrol. Earth Syst. Sci. Discuss. 20, 4819–4835.
Fauvel, B., Cauchie, H.-M., Gantzer, C., Ogorzaly, L., 2016. Contribution of hydrological data to the understanding of the spatio-temporal dynamics of F-specific RNA bacteriophages in river water during rainfall-runoff events. Water Res. 94, 328–340.
Halliday, S.J., Skeffington, R.A., Wade, A.J., Neal, C., Reynolds, N., Norris, D., Kirchner, J.W., 2013. Upland streamwater nitrate dynamics across decadal to sub-daily timescales: a case study of Plynlimon, Wales. Biogeosciences 10, 8013–8038.
Jones, T.D., Chappell, N.A., 2014. Streamflow and hydrogen ion interrelationships identified using Data-Based Mechanistic modelling of high frequency observations through contiguous storms. Hydrol. Res. 45, 868–892.
Jones, T.D., Chappell, N.A., Tych, W., 2014. First dynamic model of dissolved organic carbon derived directly from high frequency observations through contiguous storms. Environ. Sci. Technol. 48, 13289–13297.
Kirchner, J.W., Feng, X., Neal, C., Robson, A.J., 2004. The fine structure of water-quality dynamics: the (high-frequency) wave of the future. Hydrol. Process 18, 1353–1359.
Kretzschmar, A., Tych, W., Chappell, N.A., 2014. Reversing Hydrology: estimation of sub-hourly rainfall time-series from streamflow. Environ. Modell. Softw. 60, 290–301.
Langan, S.J., Whitehead, P.G., 1987. The Application of Time-series Modelling to Short-term Streamwater Acidification in Upland Scotland, vol. 167. IAHS-AIHS Publication, pp. 75–87.
Lathi, B.P., 2010. Linear Systems and Signals. Oxford University Press.
Lepot, M., Torres, A., Hofer, T., Caradot, N., Gruber, G., Aubin, J.B., Bertrand-Krajewski, J.L., 2016. Calibration of UV/Vis spectrophotometers: a review and comparison of different methods to estimate TSS and total and dissolved COD concentrations in sewers, WWTPs and rivers. Water Res. 101, 519–534.
Littlewood, I.G., 1987. Streamflow - pH dynamics in small moorland and conifer afforested catchments in the Upper Tywi valley, Wales. In: National Hydrology Symposium. University of Hull, 14–16 September 1987. Hull, UK, British Hydrological Society 23.1-23.12.
Littlewood, I.G., Croke, B.F.W., 2013. Effects of data time-step on the accuracy of calibrated rainfall-streamflow model parameters: practical aspects of uncertainty reduction. Hydrol. Res. 44, 430–440.
Ockenden, M.C., Chappell, N.A., Neal, C., 2014. Quantifying the differential contributions of deep groundwater to streamflow in nested basins, using both water quality characteristics and water balance. Hydrol. Res. 45, 200–212.
Petry, J., Soulsby, C., Malcolm, I.A., Youngson, A.F., 2002. Hydrological controls on nutrient concentrations and fluxes in agricultural catchments. Sci. Total. Environ. 294, 95–110.
Reynolds, K.N., Loecke, T.D., Burgin, A.J., Davis, C.A., Riveros-Iregui, D., Thomas, S.A., St Clair, M.A., Ward, A.S., 2016. Optimizing sampling strategies for riverine nitrate using high-frequency data in agricultural watersheds. Environ. Sci. Technol. 50, 6406–6414.
Rozemeijer, J.C., van der Velde, Y., van Geer, F.C., de Rooij, G.H., Torfs, P.J.J.F., Broers, H.P., 2010. Improved load estimates for NO3 and P in surface waters by characterizing the concentration response to rainfall events. Environ. Sci. Technol. 44, 6305–6312.
Taylor, C.J., Pedregal, D.J., Young, P.C., Tych, W., 2007. Environmental time series analysis and forecasting with the Captain toolbox. Environ. Modell. Softw. 22, 797–814.
Viviano, G., Salerno, F., Manfredi, E.C., Polesello, S., Valsecchi, S., Tartari, G., 2014. Surrogate measures for providing high frequency estimates of total phosphorus concentrations in urban watersheds. Water Res. 64, 265–277.
Wade, A.J., Palmer-Felgate, E.J., Halliday, S.J., Skeffington, R.A., Loewenthal, M., Jarvie, H.P., Bowes, M.J., Greenway, G.M., Haswell, S.J., Bell, I.M., Joly, E., Fallatah, A., Neal, C., Williams, R.J., Gozzard, E., Newman, J.R., 2012. Hydrochemical processes in lowland rivers: insights from in situ, high-resolution monitoring. Hydrol. Earth Syst. Sci. 16, 4323–4342.
Witzke, B., 1998. Bedrock geologic map of northeast Iowa. In: Iowa DNR Geological Survey Bureau. Iowa Department of Natural Resources, Iowa.
Young, P.C., 2010. The estimation of continuous-time rainfall-flow models for flood risk management. In: Walsh, C. (Ed.), Role of Hydrology in Managing Consequences of a Changing Global Environment. British Hydrological Society, Newcastle upon Tyne, pp. 303–310.
Young, P.C., 2015. Refined instrumental variable estimation: maximum likelihood optimization of a unified Box–Jenkins model. Automatica 52, 35–46.